Supplementary Information

Generic tags for Mn(II) and Gd(III) spin labels for distance measurements in proteins

Yin Yang[a,+], Yan-Jun Gong[b,+], Aleksei Litvinov[a], Hong-Kai Liu[b], Feng Yang[b], Xun-Cheng Su[b,*] and Daniella Goldfarb[a,*]

[a] Department of Chemical Physics, Weizmann Institute of Science, Rehovot, 76100 Israel, [b] State Key Laboratory of Elemento-Organic Chemistry, Collaborative Innovation Center of Chemical Science and Engineering (Tianjin), College of Chemistry, Nankai University, Tianjin 300071, China

Contents

1. Mass-spectra of the conjugated proteins.

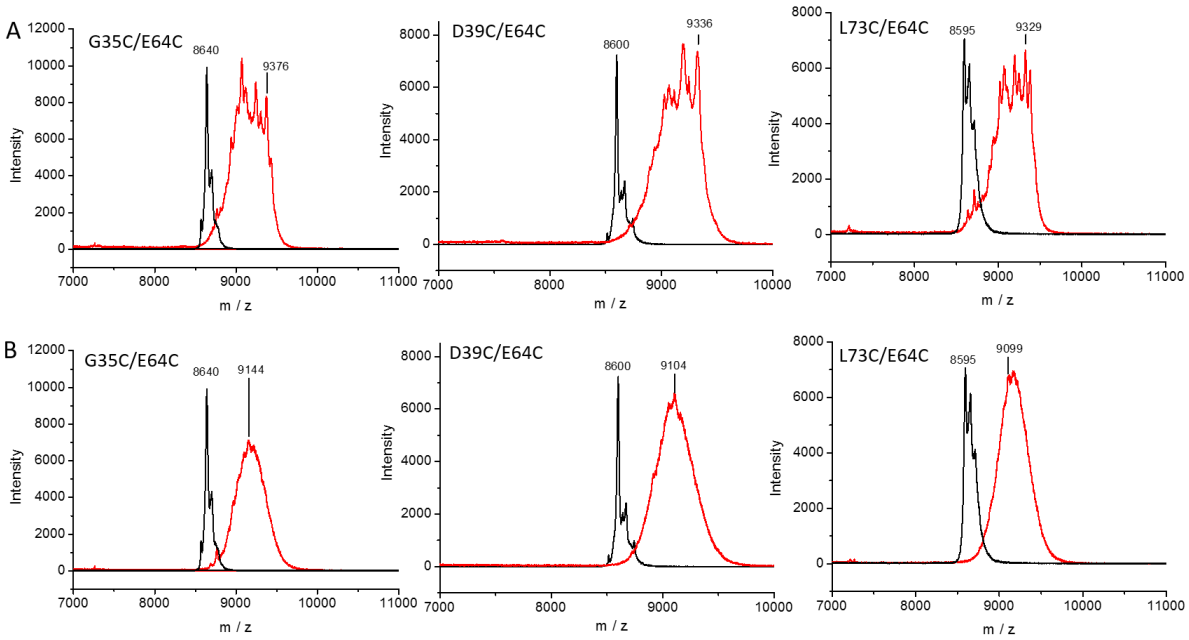

Fig. S1. MALDI-TOF mass spectra of the ubiquitin mutants (0.1 mM, unlabeled) (black) and their conjugates with the paramagnetic tag (red): (A) PyMTA; (B) PyNPDA. For the PyMTA conjugates, the calculated molecular mass difference of 736 mass units between ubiquitin and its PyMTA conjugate is identical to the difference of masses observed. It is noted that in the PyNPDA conjugates the molecular mass difference around 504 which corresponds to the release of 2-methyl nitrophenol group during the measurements of the mass spectra as shown below:

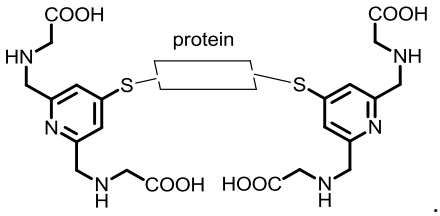

2. The binding affinity of 4PSPyNPDA

The binding affinity of 4PSPyNPDA with Gd(III) and Mn(II) was evaluated as follows: For a mixture of 20 μM [EDTA] and 20 μM 4PSPyNPDA in a 20 mM MES buffer, at pH 6.4 at 298 K, the UV absorption at 387 nm for Gd(III)) and 400 nm for Mn(II)) was measured as a function of added $Gd(NO_3)_3$ or $MnCl_2$ from 0 up to 40 μM. The association constant K_a of 4PSPyNPDA with Gd(III) and Mn(II) was obtained using the known K_d, dissociation constant, of EDTA with Gd(III) (10^{-17} M) and Mn(II) ($10^{-13.58}$ M) , following the established protocol according to eq. (1).[1]

$K_dK_a = ([L]_{total}/[M\text{-}L] -1)/([EDTA]total/[M\text{-}EDTA] -1)$ (1)

where M represents the metal ion (Gd(III) or Mn(II)) and L the 4PSPyNPDA ligand, K_d is the dissociation constant of M-EDTA and K_a is the apparent association constant of M-L under the experimental conditions used. The determined K_a values for 4PSPyNPDA with Gd(III) and Mn(II) are 2.3×10^{17} M^{-1} and 7.2×10^{13} M^{-1}, respectively; higher than that of EDTA. The results are shown in Fig. S2.

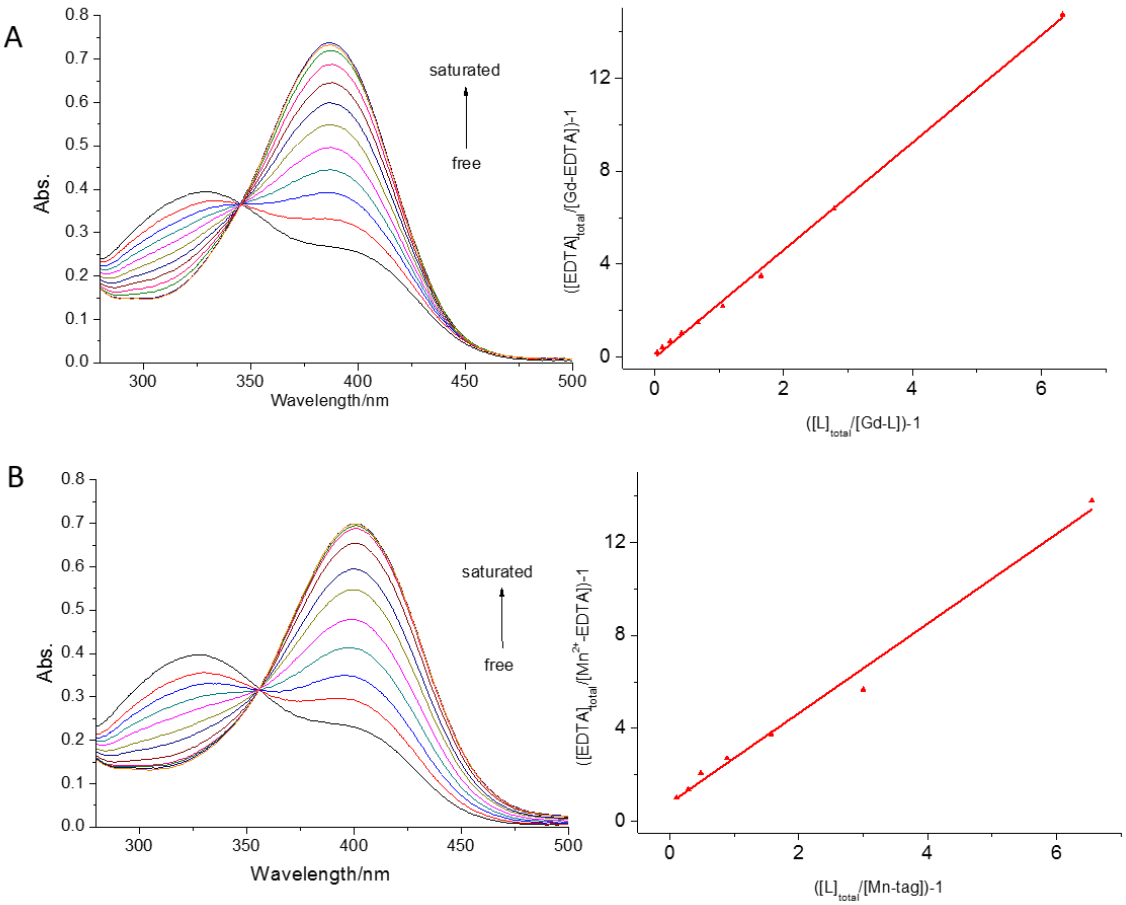

Fig. S2. Determination of association constant of 4PSPyNPDA with Gd(III) (A) or Mn(II) (B) using competition experiment in the presence of EDTA. The UV-vis spectra are shown on the left and the plot of eq. (1) for effective competition for Gd(III) or Mn(II) between 4PSPyNPDA and EDTA on the right. The slops for Gd(III) and Mn(II) are 2.3 and 1.9, respectively.

3. The effect of the tags on the NMR chemical shifts.

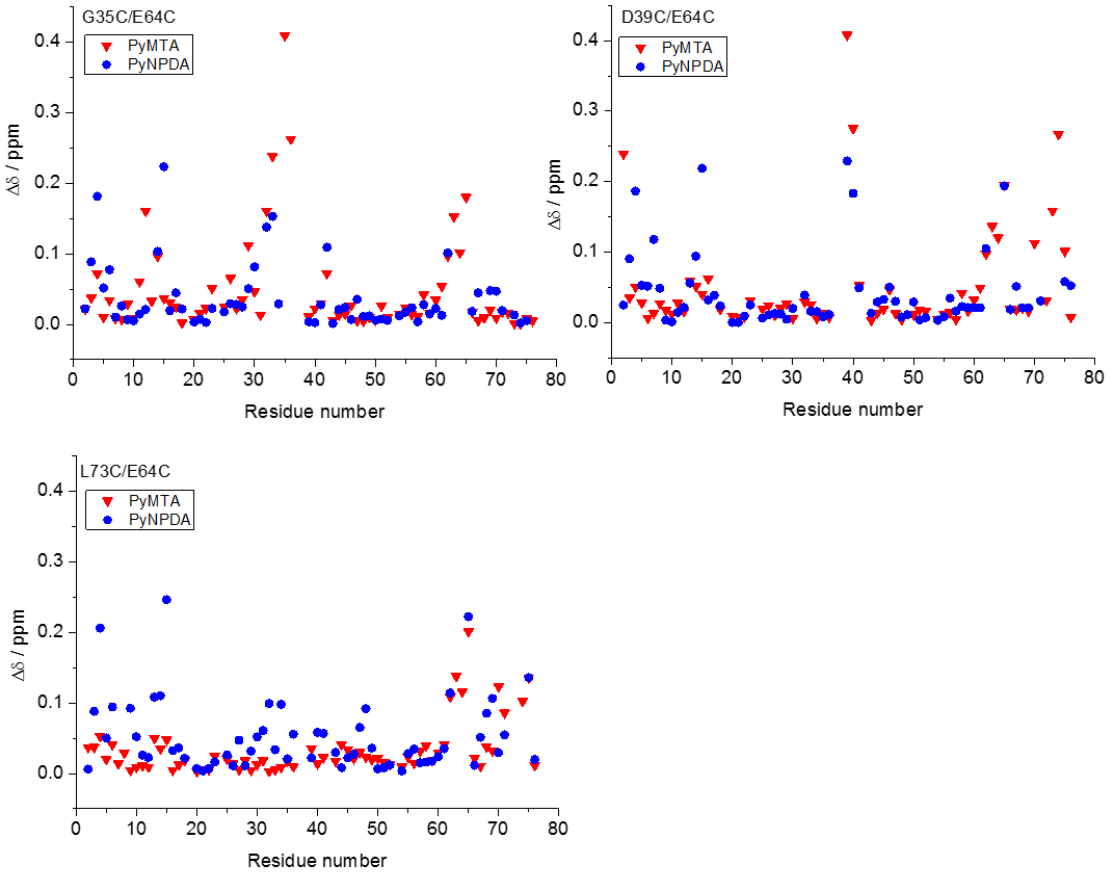

Fig. S3. Chemical shift changes between the ubiquitin mutant and its dual labeling adduct with the paramagnetic tags. Chemical shift differences were calculated as $\Delta\delta = \mathrm{Sqrt}[(\Delta\delta_H)^2 + (\Delta\delta_N/10)^2]$, where $\Delta\delta_H$ and $\Delta\delta_N$ are the backbone amide chemical shift differences in the hydrogen and nitrogen dimension, respectively.

4. ED-EPR spectra

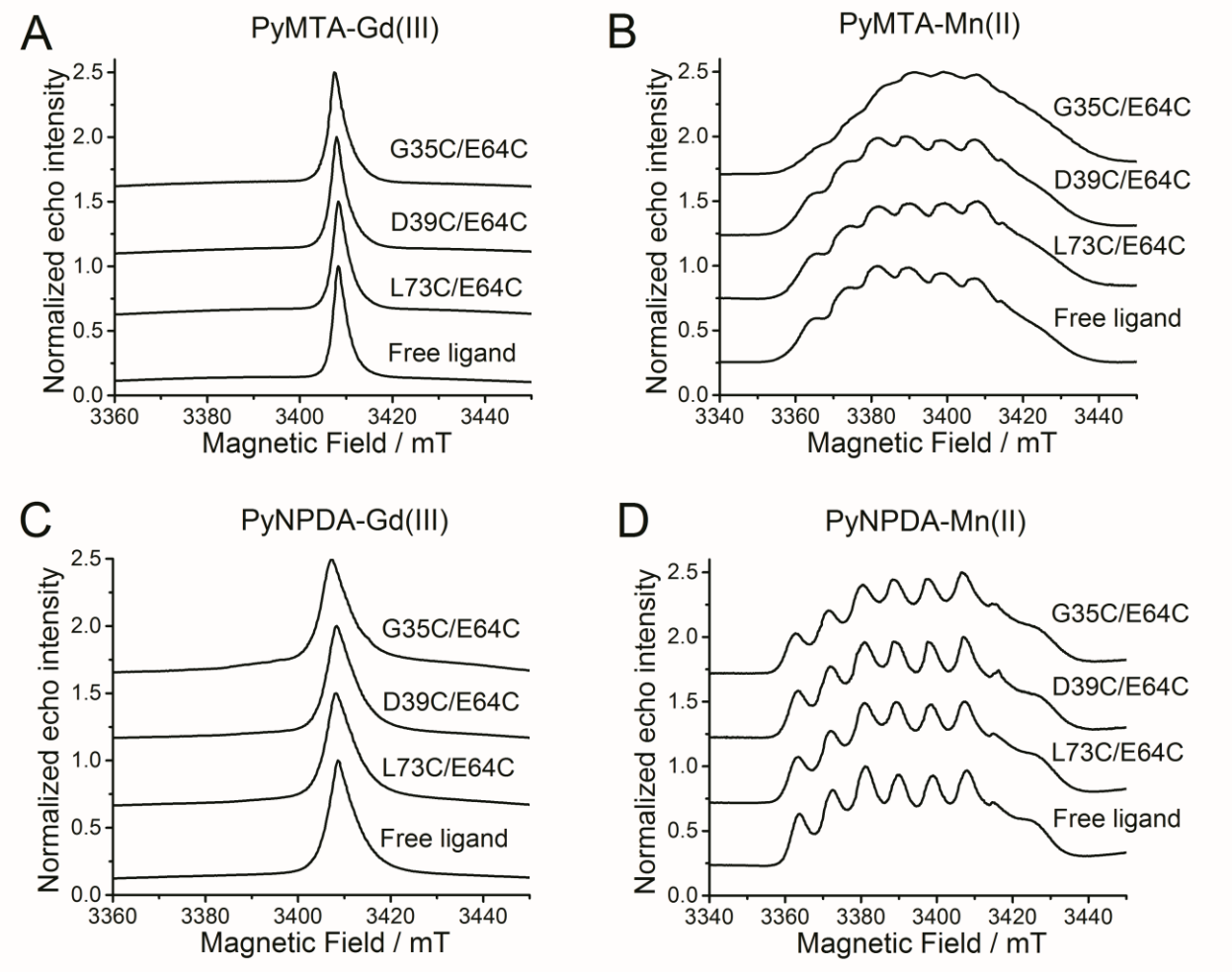

Fig. S4. W-band ED-EPR spectra of ubiquitin mutants coubly labelled with PyMTA-Gd(III) (A), PyMTA-Mn(II) (B), PyNPDA-Gd(III) (C) and PyNPDA-Mn(II) (D). In each panel the bottom trace corresponds to the free tag.

5. Echo decay curves

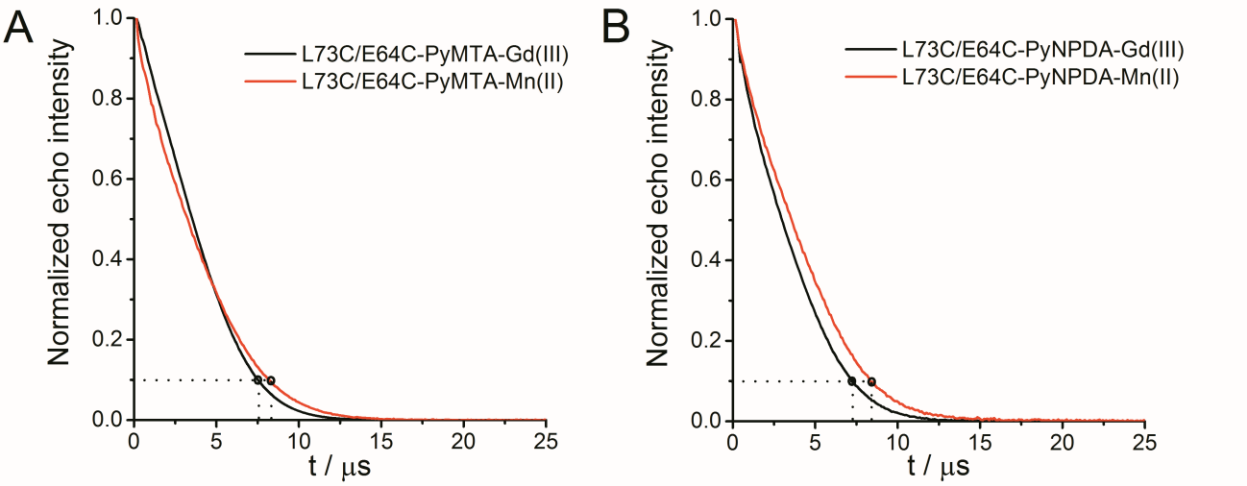

Fig. S5. Two pulse-echo decay of ubiquitin L73C/E64C doubly labelled with (A) PyMTA-Gd(III) (black) and PyMTA-Mn(II) (red); (B) PyNPDA-Gd(III) (black) and PyNPDA-Mn(II) (red) recorded at the maximum of the ED-EPR spectra. The open circles represent the echo at 10% of its maximum intensity.

Table S1. Summary of the $\tau_{10\%}$ values of all samples studies.

sample	PyMTA-Gd(III) (μs)	PyMTA-Mn(II) (μs)	PyNPDA-Gd(III) (μs)	PyNPDA-Mn(II) (μs)
Free ligand	8.1	8.2	8.0	8.9
G35C/E64C	7.9	7.6	7.2	8.3
D39C/E64C	7.6	7.9	7.3	8.2
L73C/E64C	7.5	8.1	7.3	8.4

6. Primary DEER data, distance distributions with validations and L-curves

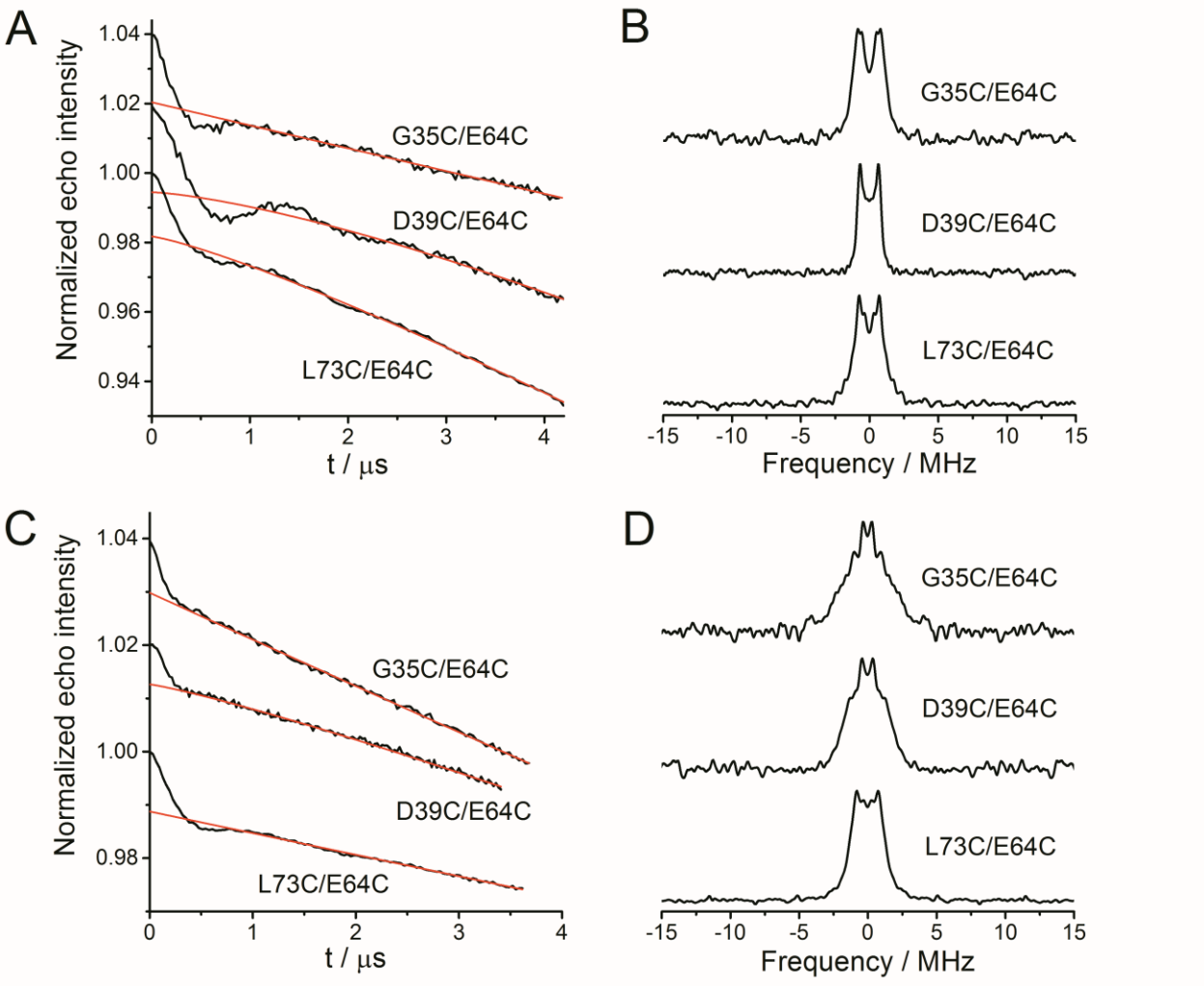

Fig. S6. W-band primary DEER results, with the background decay function, of the ubiquitin mutants doubly labelled with PyMTA-Gd(III) (A) and PyMTA-Mn(II) (C); (B, D) The corresponding Fourier transforms of the DEER data after background removal.

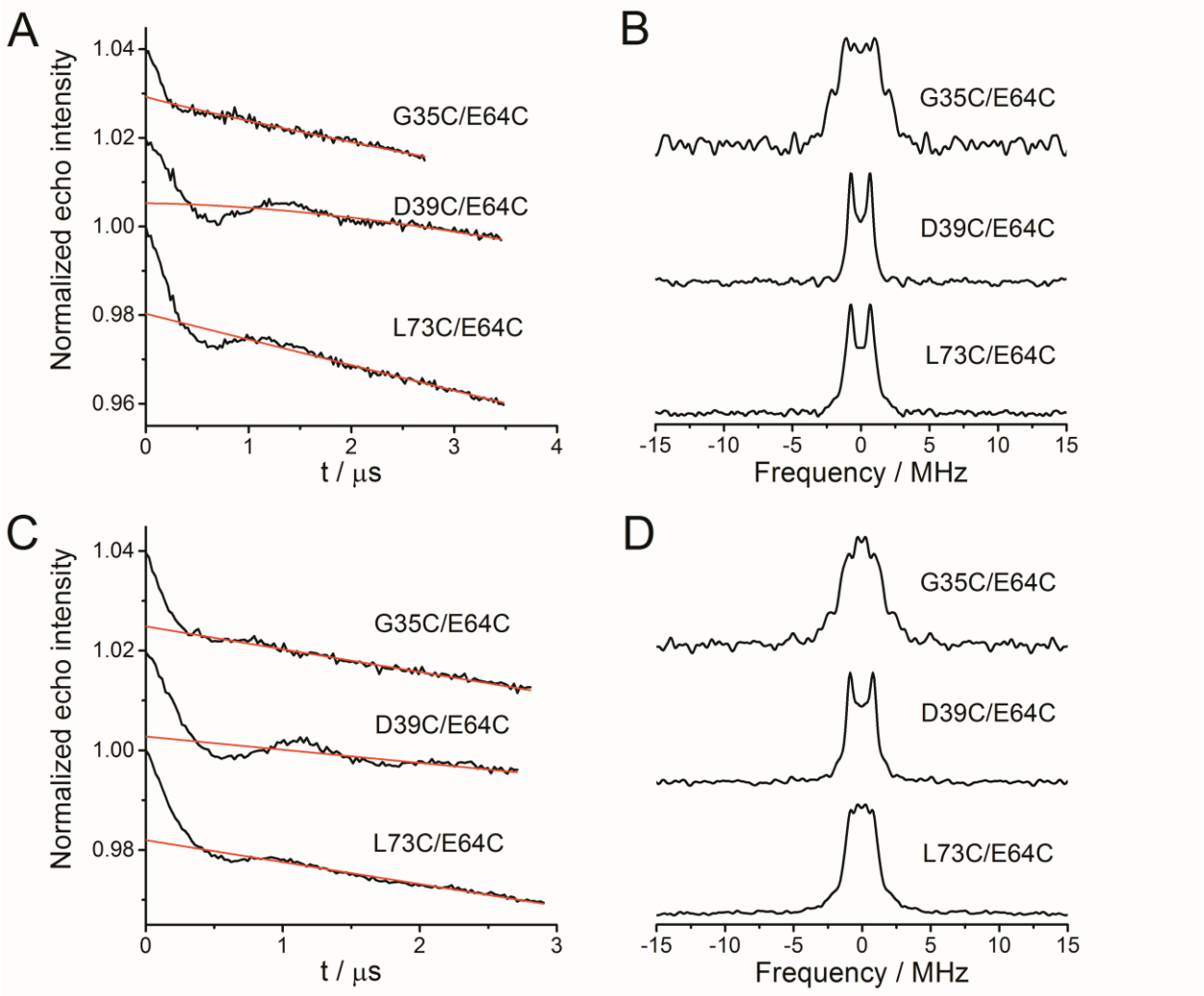

Fig. S7. W-band primary DEER results with the background decay function the ubiquitin mutants doubly labelled with PyNPDA-Gd(III) (A) and PyNPDA-Mn(II) (C); (B, D) The corresponding Fourier transforms of the DEER data after background removal.

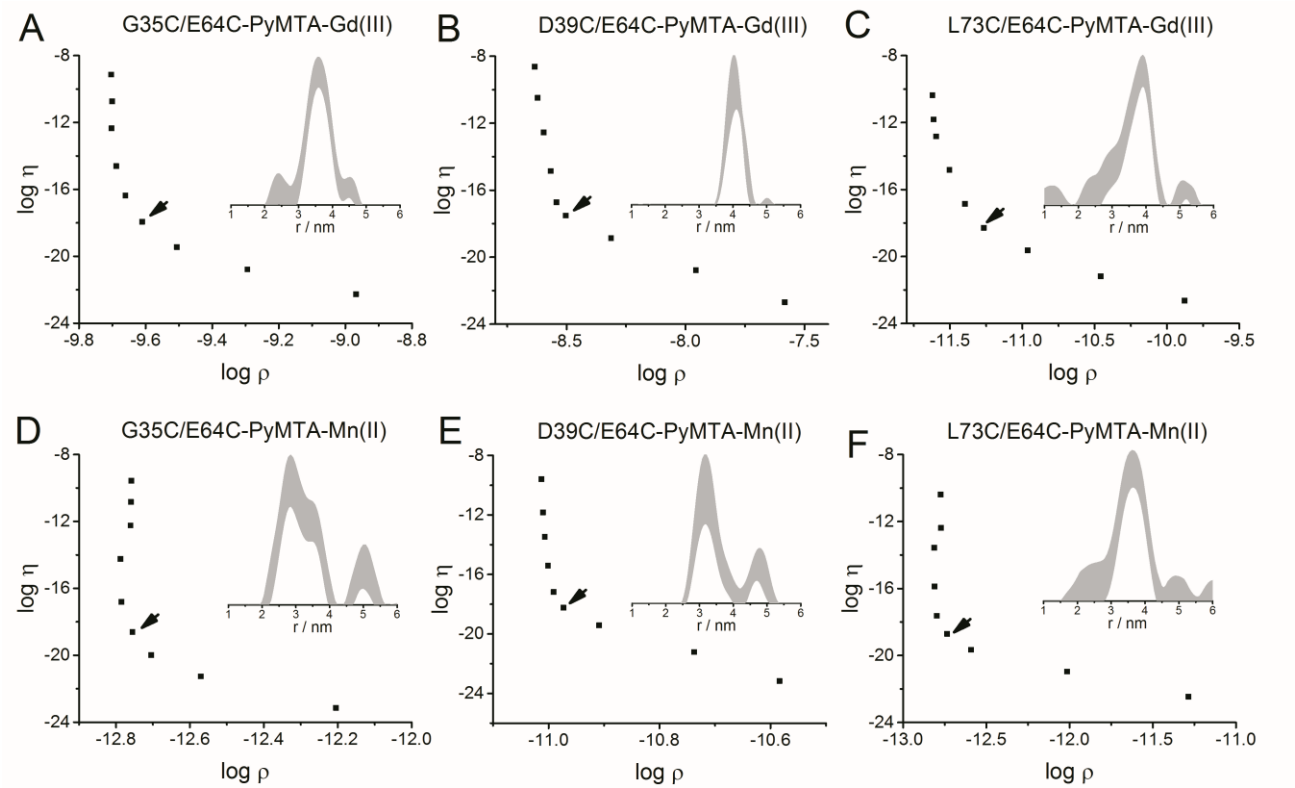

Fig. S8. Distance distributions (inserts) of the ubiquitin mutants doubly labelled with PyMTA-Gd(III) (top raw) and PyMTA-Mn(II) (bottom raw) with the uncertainty range as obtained using the validation procedure of DeerAnalysis[2] along with the associated L-curve with the chosen Tikhonov regularization parameter α indicated by an arrow.

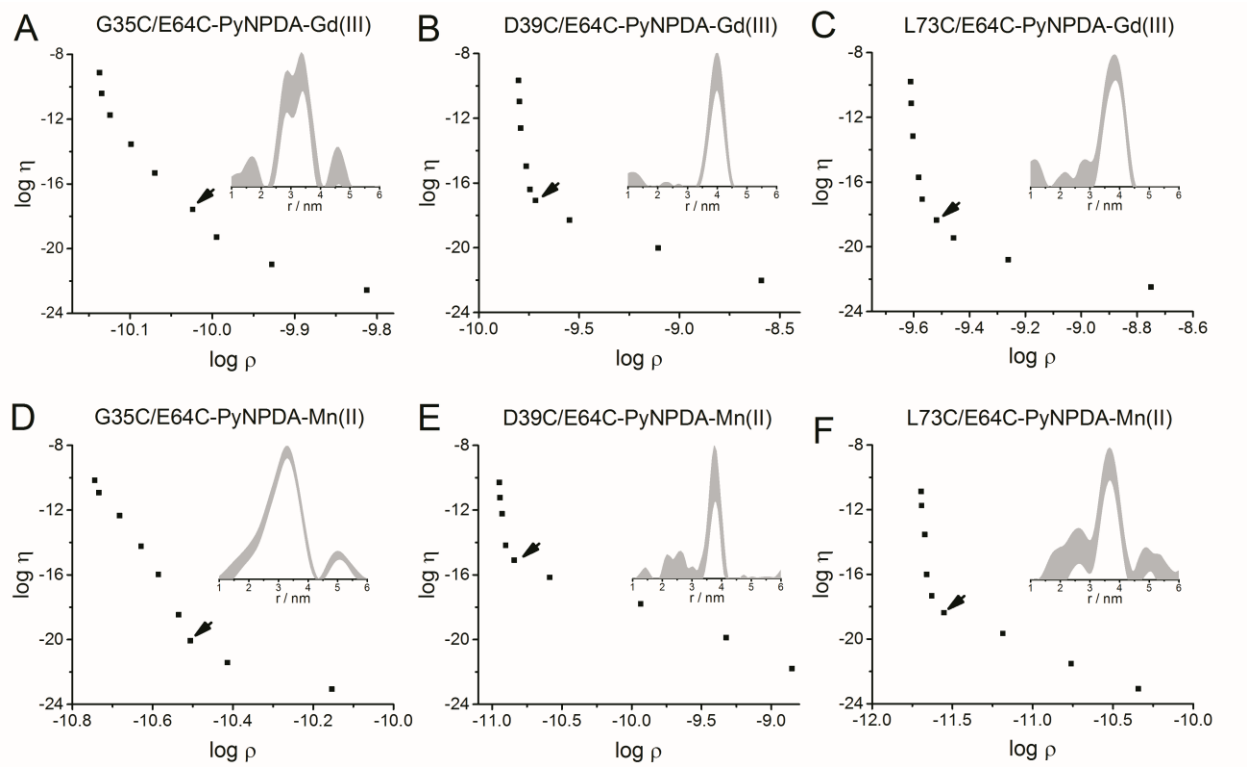

Fig. S9. Distance distributions (inserts) of the ubiquitin mutants doubly labelled with PyNDPA-Gd(III) (top raw) and PyNDP-Mn(II) (bottom raw) with the uncertainty range as obtained using the validation procedure of DeerAnalysis along with the associated L-curve with the chosen Tikhonov regularization parameter α indicated by an arrow.

7. ELDOR-detected NMR and ENDOR results.

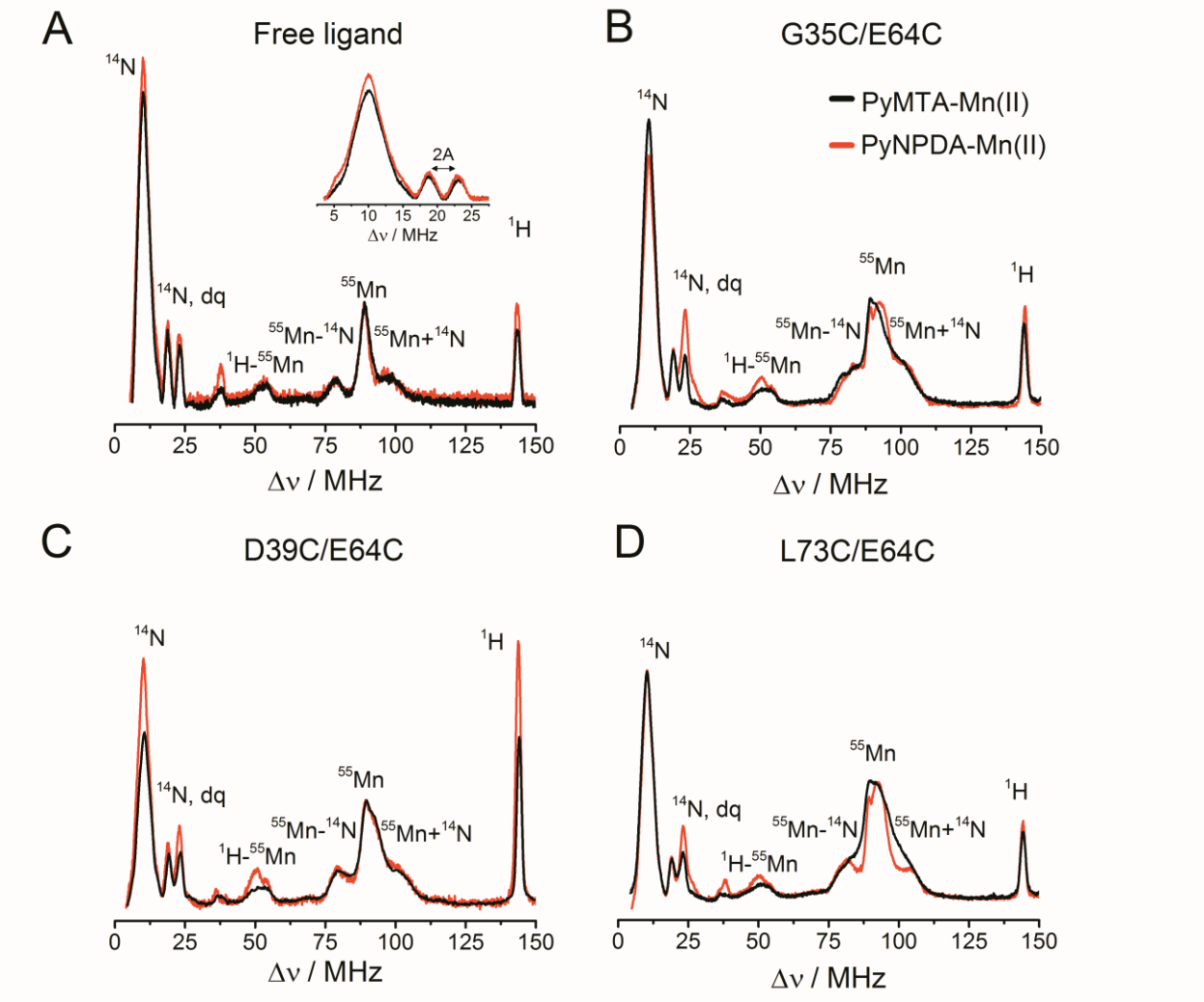

Fig. S10. W-band EDNMR spectra of 4PSPyMTA-Mn(II) and 4PSPyNPDA-Mn(II) (A) and the doubly labelled ubiquitin mutants (B, C,D). The inset in A is a zoom on the ^{14}N region with the splitting of the two double quantum transitions, which yields the hyperfine coupling, *A*. The spectra are shown after background subtraction and multiplication of the intensities by -1 and were normalized to the ^{55}Mn signal.

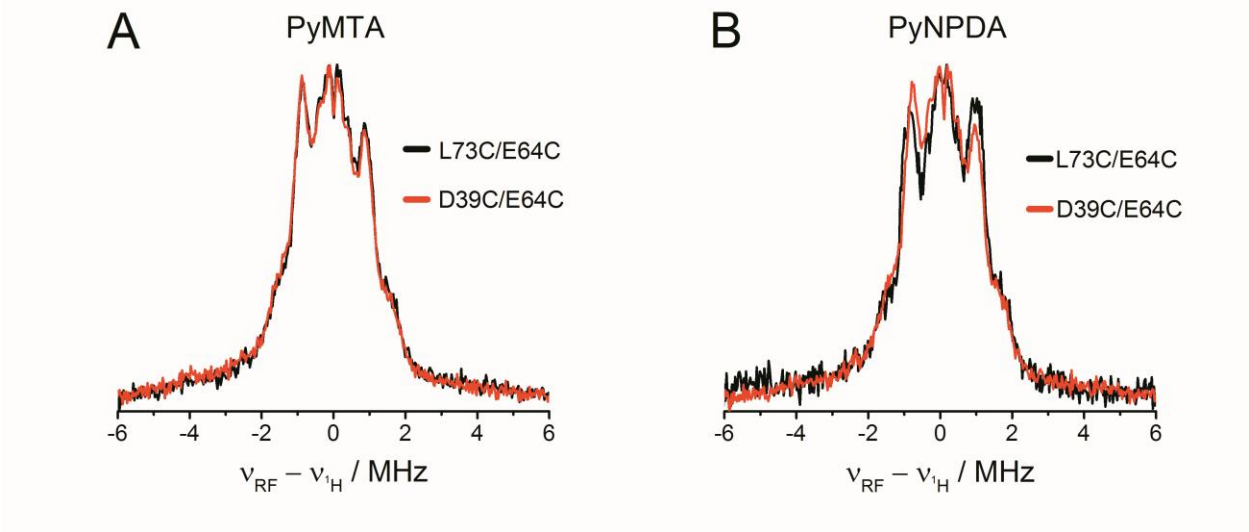

Fig. S11. W-band ^{1}H Davies ENDOR of L73C/E64C PyMTA- Mn(II) and D39C/E64C PyMTA- Mn(II) (A) and L73C/E64C PyNDPA- Mn(II) and D39C/E64C PyNDPA- Mn(II). All samples were in H_2O/glycerol (7:3).

8. Calculated distance distributions

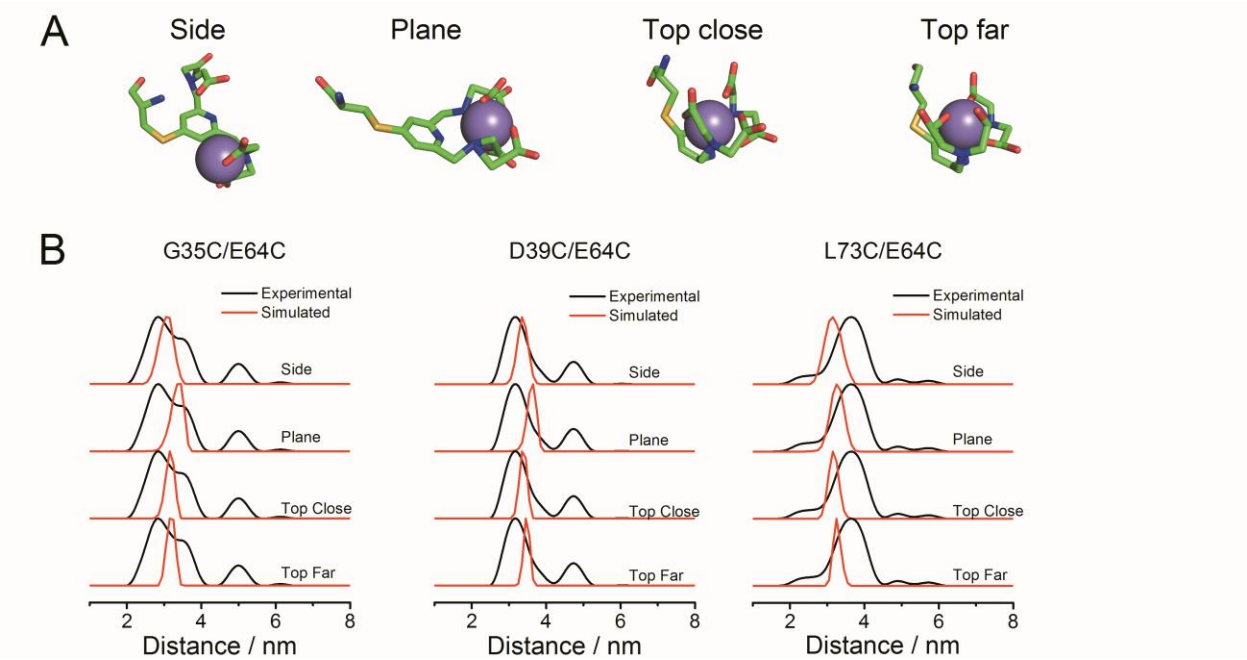

Fig. S12. (A) The four hypothetical coordination modes of Mn(II) with the protein bound PyMTA tag . The "Plane" configuration, where the Mn(II) is in the plane of the pyridine, was produced from the PyMTA-Gd(III) structure by replacing Gd(III) with Mn(II) and removing the Mn(II) bond to the pyridine nitrogen. Upon geometry optimization with MM scripts this resulted in slight shift of Mn(II) position in the complex relative to Gd(III). The Mn-N and Mn-O bond lengths were all in the 1.8-1.9 Å range. The "Top" configurations were constructed by fixing the Mn(II) atom above the pyridine ring while letting the *N*-Bis (carboxylmethyl) arms free to find a position with some local minimum energy. This generated for the Top-Close structure Mn-N and Mn-O bond lengths of 2.4-2.5 Å and for the Top-Far configuration Mn-O lengths of 1.8 Å and Mn-N lengths of 2.8-2.9 Å. Finally the "Side" configuration represents the case when Mn(II) is only coordinated to one of the *N*-Bis (carboxylmethyl) chains arms of PyMTA and is open for interaction with solvent, or surrounding residues of the protein. Here the Mn-N and Mn-O bond lengths were 1.8 Å. (B) The calculated distance distribution for each of the coordination modes shown in A as compared to the experimental data for the three double mutants studied. For reference, the crystal structure of Mn(II)EDTA , where the Mn(II) is coordinated to an additional water molecule reports on Mn-O bonds of 2.236 Å and Mn-N of 2.377 Å.[3]

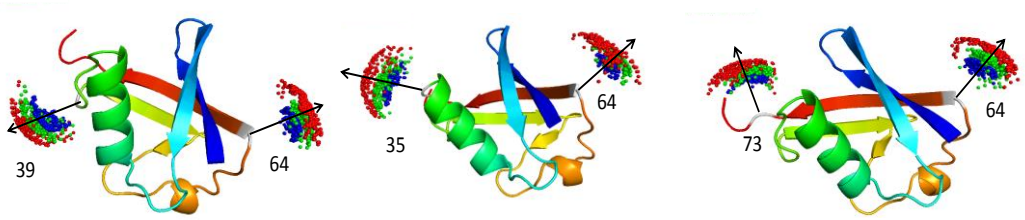

Fig. S13. The location of Gd(III) (red) and Mn(II) in the in the "Plane" configuration (green) and "Top-close" configuration (blue) for the three studied mutants labeled with PyMTA (left D39C/E64C, middle G35C/E64C, right L73C/E64C). The arrows point to the approximate direction of the cone produced by the metal ion locations showing the relative orientations of the two cones in each mutant. The cones in D39C/E64C (left) have an orientation that is expected to show the highest shift in the distance distribution between Gd(III) and Mn(II), whereas for L73C/E64C (right) they have the an orientation that displays the least sensitivity to the metal location.

9. Comparison with PyEDTA distance distribution.

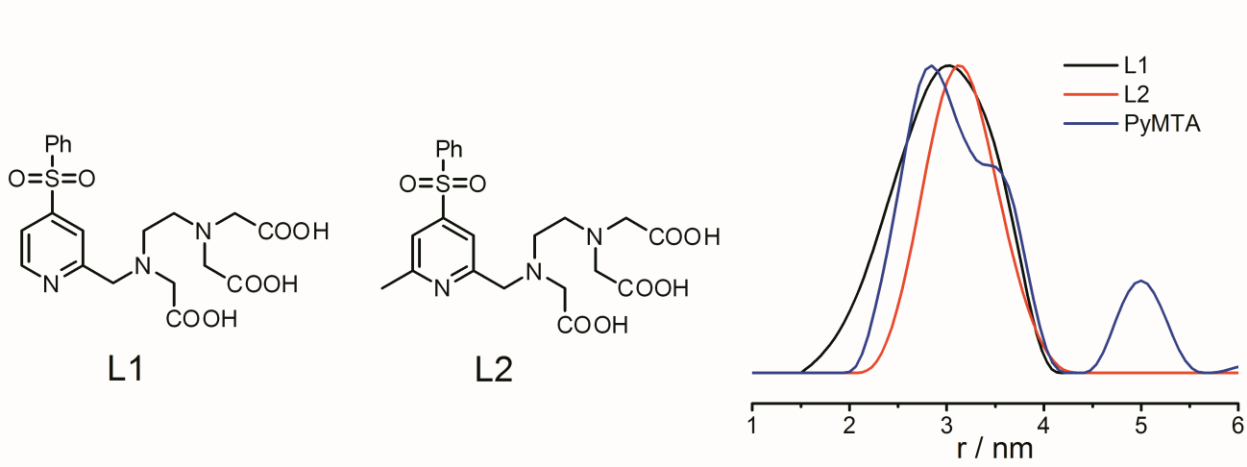

Fig. S14. The chemical structures of the L1 and L2 tags along with the distance distribution of ubiquitin G35C/E64C mutated labelled with these tags[4] and Mn(II) compared with the corresponding distance distribution obtained with PyMTA-Mn(II).

10. PRE maps of ubiquitin-PyMTA with Gd(III) and Mn(II).

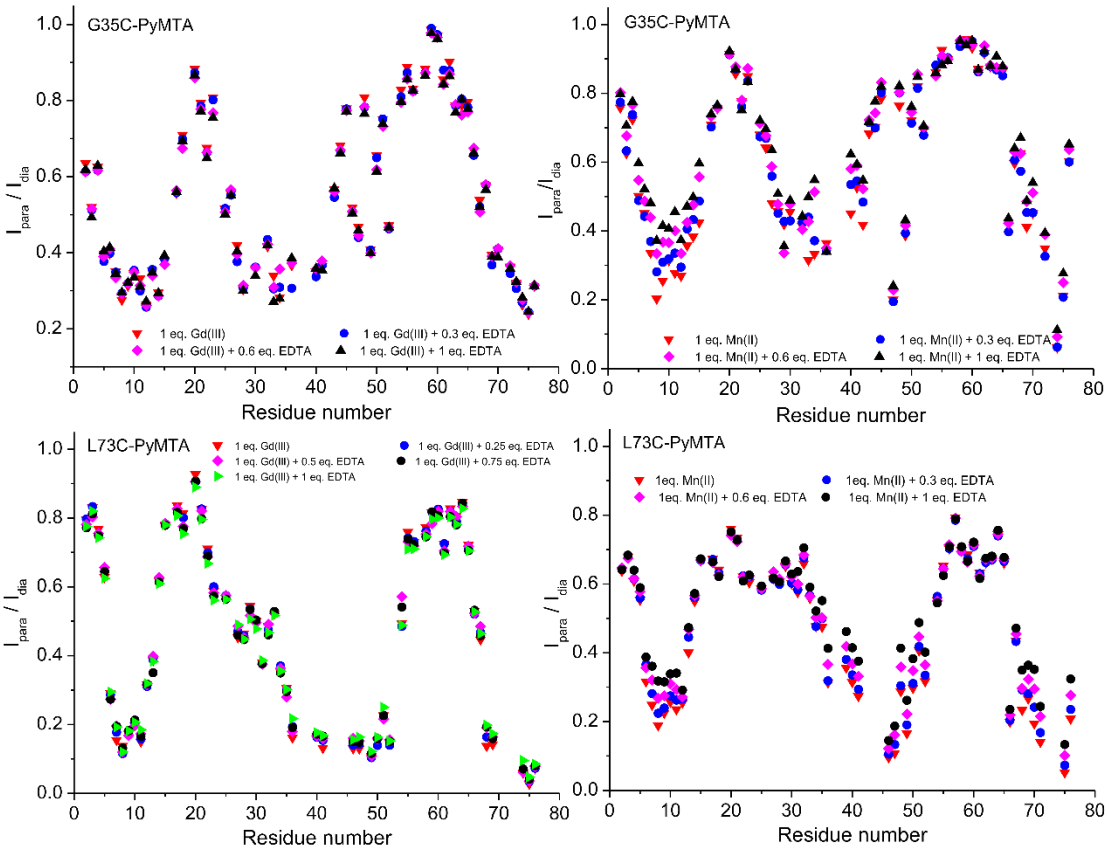

Fig. S15. PRE analysis of ubiquitin-PyMTA in the absence and presence of Mn(II) or Gd(III). I_{dia} represents the cross-peak intensity in the ^{15}N-HSQC spectrum recorded for the sample of free ubiquitin-PyMTA in 20 mM MES buffer at pH 6.4 and 298 K, I_{para} represents cross-peak intensity of the above samples with addition of paramagnetic metal ion or paramagnetic ion and EDTA.

References:

1. L. Zhang, M. Koay, M. J. Maher, Z. Xiao and A. G. Wedd, *J. Am. Chem. Soc.*, 2006, **128**, 5834-5850.
2. G. Jeschke, V. Chechik, P. Ionita, A. Godt, H. Zimmermann, J. Banham, C. R. Timmel, D. Hilger and H. Jung, *Appl. Magn. Reson.*, 2006, **30**, 473-498.
3. S. Richards, B. Pedersen, J. V. Silverton and J. L. Hoard, *Inorg. Chem.*, 1964, **3**, 27-33.
4. A. Martorana, Y. Yang, Y. Zhao, Q.-F. Li, X.-C. Su and D. Goldfarb, *Dalton Trans.*, 2015, **44**, 20812-20816.